

Image Quality Estimation in Wireless Multimedia Sensor Networks: An Experimental Study

Pinar Sarisaray Boluk¹, Kerem Irgan²,
Sebnem Baydere², and A. Emre Harmanci¹

¹ Istanbul Technical University, Istanbul, Turkey
pinar.sarisaray@bahcesehir.edu.tr, harmanci@itu.edu.tr

² Yeditepe University, Istanbul, Turkey
{sbaydere,kirgan}@cse.yeditepe.edu.tr

Abstract. Multimedia applications in wireless sensor networks (WMSN) have stringent quality of service (QoS) requirements. In this paper, we study image quality distortions due to packet losses in multi hop WMSN. An experimental simulation and real testbed environment has been setup to estimate the quality of the test images over 30,000 transmissions. Two scenarios are considered: in the first scenario, images are watermarked with their replicas at the source node and an error concealment (EC) algorithm is employed at the sink. In the second scenario, raw images are transmitted without any encoding. The empirical results have revealed that there is a strong correlation between Peak-Signal-To-Noise-Ratio (PSNR) values of the distorted images and packet loss rate of the transmission route (PER). Moreover, the relationship is linear when EC technique is used with an achievement over 25dB PSNR for PER less than 0.6. This correlation is useful when designing QoS based transport schemes.

Keywords: Image Transmission, Wireless Multimedia Sensor Networks, WSN, TestBed, PSNR Estimation, Error Concealment, Watermarking.

1 Introduction

With the wireless multimedia sensor networks coming of age, a new field of research is to investigate the use of multimedia sensors to monitor and transmit data in the form of image, video and audio. That is, many applications necessitate efficient multimedia communication in sensor networks [1]. Due to strict energy constraints of sensor nodes, majority of the studies are focused on energy efficiency [2,3,4,5,6,7,5,8,9,10]. In [8], the authors present energy cost comparisons associated with transmission of raw and jpeg compressed images for a variety of processor-radio combinations. Their results show that depending on the processor-radio combination, both compressed and uncompressed image transmission schemes may be among the most energy and time efficient

options. Moreover, works in [11] demonstrate that the complexity of popular image compression algorithms may lead to greater energy consumption than the transmission of the uncompressed image.

When transmitting images over WMSN the quality is constrained by packet losses due to failures and transmission errors. Even more, cumulative packet loss rate grows exponentially with respect to number of hops in multi hop settings. Packet loss tolerance of an image coded with classical compression algorithms (e.g., JPEG, JPEG2000, SPIHT) is very low [9]. Hence, in order to achieve required perceptual quality, reliable transport protocols, such as ARQ [12] or FEC [13] are needed at the intermediate nodes to deal with packet losses [14]. However, these transport schemes may not be suitable for WMSN due to their consequent delay and additional resource requirements. In this respect, error concealment (EC) approach has received particular attention as an effective mechanism that reconstructs the distorted multimedia data as closely as the original one without increasing the bandwidth demand as well as avoiding the burden of retransmissions and consequent delay [15]. Consequently, EC algorithms are promising candidates to alleviate packet losses due to errors and failures in WMSNs. In [16], we have shown that EC algorithm gives better delay and processing performance than FEC and ARQ methods in WMSN.

In this work, we elaborate on the effectiveness of the error concealment technique for the estimation of image quality in terms of PSNR. In spite of many studies related to energy efficiency, to the best of our knowledge, image quality performance and the impact of multi hop in WMSN is not well studied in the literature.

PSNR is a full reference metric which identifies the degree of distortions in an image by comparing the pixel values with the corresponding values in the original image. However, in networked multimedia applications, in order to measure the quality of the transmitted image, the original may not be available for referencing at the sink. The motivation behind this study is to find a correlation between a measurable network parameter; ie. dropped packets rate; and the PSNR value of the transmitted image so that the quality can be estimated at the sink.

A comprehensive set of simulations are carried out in two different settings; In the first setting, the EC algorithm is used for quality enhancement. In the second, raw images are simply transmitted without any encoding. The performance of these schemes is analyzed for singlepath and disjoint multipath transmission scenarios. The simulation results are also validated in a real testbed, which is shown in Figure 2.

The results indicate that there is a promising theoretical relationship between cumulative packet loss rate (PER) over the transmission path and the quality of the degraded image in terms of PSNR. Moreover, PSNR values are linearly correlated with PER when EC technique is used. Since mapping an application quality metric to a network parameter is useful when designing QoS algorithms, we believe that this relationship is worth for further investigation. The rest of the paper is organized as follows: Section 2 introduces the system model and the EC algorithm. Section 3 gives the analysis of transmission schemes in terms of

packet loss rate. Section 4 describes simulation methodology. Section 4.1 present quality estimation results. Section 4.2 presents the performance analysis and real testbed results. Finally, Section 6 concludes with discussions and future work.

2 System Model

Figure 1 depicts the considered system, entailing two types of sensors; Type 1 $C_i, i=1, 2 \dots W$ sensors are equipped with camera and Type 2 $S_{ij}, i=1, 2 \dots W_1, j=1, 2 \dots W_2$, sensors are simple routing sensors. C_i 's and the sink's capability is higher than that of the S_{ij} 's in terms of energy, processing power, and storage capacity. $N_1 \times N_2$ 8-bit grayscale images are partitioned into $s \times s$ pixel macro-

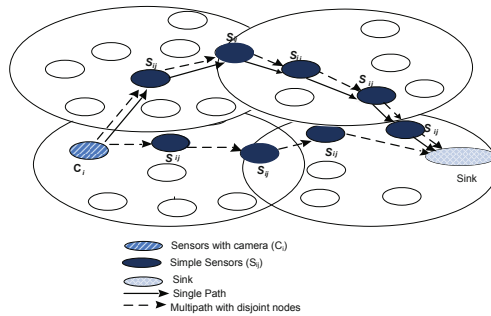


Fig. 1. General WMSN scenario

blocks at the source node. Each macro-block is transmitted in a separate network packet towards the sink over a single path or disjoint multipath. So the number of distinct data packets to be transmitted are $N = N_1 \times N_2/s^2$ per image. Two construction schemes are considered: in the first scheme, the images are transmitted in their raw form (NC) and in the second, images are encoded using the following error concealment (EC) algorithm.

2.1 EC Algorithm

The EC algorithm ¹ employs a modified discrete wavelet transform (DWT) for embedding downsized replicas of original image into itself, thereby mitigating degradations in a backward-compatible scheme without increasing the total size of the data to be transmitted. Additionally, it corrects pixel and block losses due to transmissions using embedded replicas. We embed the replicas of the original

¹ An earlier version of this algorithm was presented at the 2007 IEEE/ACM International Symposium on Modelling, Analysis and Simulation of Computer and Telecommunication Systems (MASCOTS 2007) in part and was published in its proceedings.



Fig. 2. A view from testbed area

image's $M \times M$ macro-blocks in the sub-bands of the to-be-transmitted image, excluding LL (low-low) sub-bands, in order to limit the visual degradation. The host macro-blocks where replicas are embedded are chosen by using a shared-key-dependent pseudo-random sequence, so the extraction of the replicas is blind. If all of the replicas embedded in the sub-bands are lost, then each pixel in the lost macro-block is replaced by the median value of the sequence composed of non-zero values of neighboring macro-blocks' corresponding pixel. The detailed algorithm can be described as follows:

At the Source Nodes C_j ,

1. Capture the original image, I , with size of $N_1 \times N_2$ pixels.
2. If there are macro-blocks consisting of all 0's, then replace a pixel value in each of these macro-blocks with 1. This step facilitates fragile watermarking for error detection, and is inspired by work of Kundur et al [17].
3. Take l^{th} level pyramid-structured DWT of the original image I . Note that $k \geq l$, where k is the number of levels of the tree structured DWT.
4. Store each $(M/2^k) \times (M/2^k)$ macro-block of the tree structured DWT of the original image, namely replicas.
5. Scale each replica by the designated coefficient, then embed that scaled replica in each pyramid-structured wavelet sub-band, excluding LL ones, by using shared-key dependent sequence for each individual sub-band. Note that step 4 to 6 actualizes robust watermarking schema, which uses repeated watermark technique which is a modified version of the method studied by Kundur et al. [18].

6. Take inverse DWT (IDWT) of the watermarked image, namely IWM, and round the floating-point pixel values to the corresponding integer values.

At the Sink,

1. Read the received image, I_{rec} , and determine the lost pixels by searching blocks consisting of 0's. Thus, we utilize fragile watermarks in this step for error-detection.
2. Take l^{th} level pyramid-structured DWT of the received image I_{rec} .
3. By generating shared-key dependent random sequence, which was also used in the encoder, determine the location of lost pixels' replicas for each individual sub-band.
4. Multiply each replica with the known scaling coefficient used in encoder and take k^{th} level IDWT of the extracted replicas.
5. If there is more than one non-zero extracted pixels, take average of all those non-zero values, then place that average into the received image, I_{rec} , as the lost pixels. After this process is finished, the extracted image, I_{ext} is constructed.
6. Scan I_{ext} for lost blocks, which could not be healed. If there are still blocks consisting of all 0's, then replace them with the median value of the neighboring healthy blocks. After this process, the healed image I_{healed} is constructed in the sink.

2.2 Image Quality

In this study, image quality is measured as the mean squared error (MSE) value which is defined as

$$MSE = \frac{1}{N_1 \times N_2} \sum_i^{N_1} \sum_i^{N_2} [I(i, j) - \hat{I}(i, j)]^2 \quad (1)$$

where $I(i, j)$ and $\hat{I}(i, j)$ are the pixel values of the original and reconstructed images respectively. We use the following PSNR metric which is

$$PSNR(dB) = 20 \log_{10} \frac{2^n - 1}{\sqrt{MSE}} \quad (2)$$

where $n = 8$ for 8-bit grayscale images and $(2^n - 1)$ is the largest possible value of the signal.

3 Image Transmission Model

In this section, we provide an analysis of the packet loss rate (PER) for single path and disjoint multipath transport schemes in multi hop network.

Disjoint multipath transmission is employed to provide fault tolerance at the expense of increased bandwidth usage and processing overhead. In this scheme, captured images are transmitted through diverse paths to improve the perceptual quality of the received image at the sink. Disjoint multipath transmission scheme constructs n_p disjoint paths ($n_p = 2$ in our case). These parallel streams may independently suffer from node failures and channel impairments. Therefore, received redundant images may include both lost and correct pixel values. However, the likelihood of simultaneous losses on all paths is lower than losses on a single path. This probabilistic leverage facilitates an additional robustness of multipath transmission. Disjoint multipath scheme also utilizes a simple fusion algorithm namely *select max* on the sink. The algorithm performs fusion in the pixel value domain by selecting for each fused pixel the input coefficient with the largest absolute value. The block diagram of this operation is depicted in Figure 3.

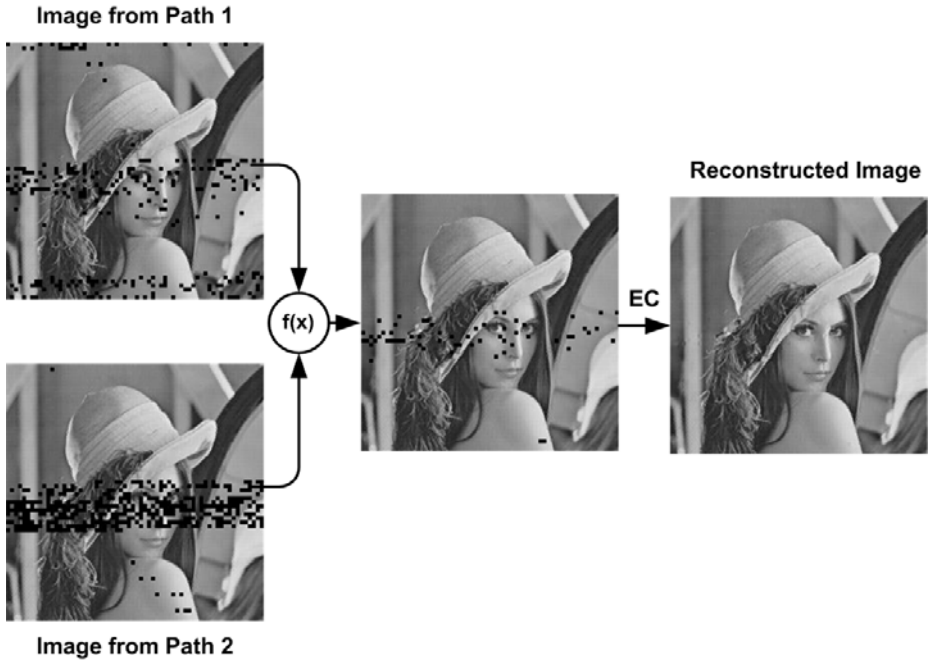


Fig. 3. An illustration of Error Concealment over Disjoint Multipath (ECDP)

3.1 Packet Loss Analysis

First, we start with the analysis of the simplest case, where there is a transmission over two parallel paths of two hops as depicted in Figure 4. For this case, packet loss means that the packet is lost on both paths. The packet carrying an image block is either lost on the first hop, which gives p , or it is not lost on the first

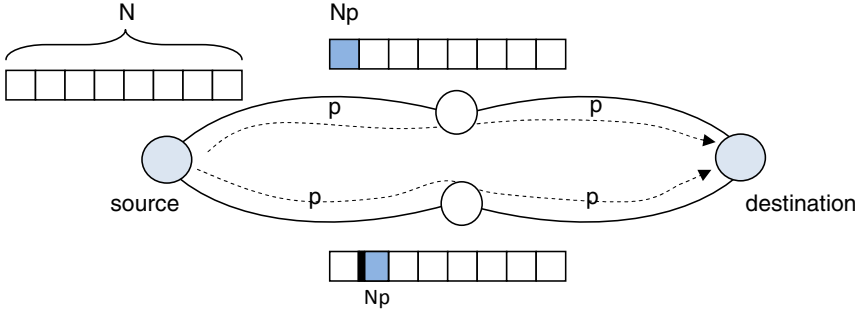


Fig. 4. Multipath transmission using two parallel paths

hop but lost on the second hop, which gives $(1 - p)p$. Adding these probabilities, we get

$$PER_1^2 = (p) + ((1 - p)p) = 2p - p^2 \tag{3}$$

PER_1^2 corresponds to the probability of loss over *two* hops for the *single* path case. We should multiply this probability by itself since we need to have simultaneous failures in two paths case. This yields:

$$PER_2^2 = (2p - p^2)^2 \tag{4}$$

Generalizing the above analysis, for n_p paths each with n_h hops we get

$$PER_{n_p}^{n_h} = [1 - (1 - p)^{n_h}]^{n_p} \tag{5}$$

Hence, if we have N Blocks transmitted from the source towards the sink, the number of lost blocks x will be given as

$$x = N \cdot [1 - (1 - p)^{n_h}]^{n_p} \tag{6}$$

4 Experimental Setup

We established an experimental setup to analyze the image quality for three transport variants:

1. No error concealment (NC)
2. Error Concealment over single path (EC)
3. Error Concealment over disjoint multipath (ECDP).

Scheme (I) is the simplest case selected as a baseline for performance improvement. In this scheme, we consider transmitting 256×256 pixels grayscale raw images tiled with 4×4 macro-blocks from source to destination on a single path, subject to certain channel and radio impairments. Scheme (II) employs the error

concealment algorithm on a single path. Scheme (III) employs the error concealment algorithm on two disjoint paths. In this scheme, a simple fusion algorithm is applied to the replicas at the sink.

To study the effect of the physical layer on the quality of the transmitted image we assumed a log log-normal shadow fading channel using NRZ encoding and NCFSK modulation as proposed in [19]. From the model, packet error rate p for distance d is obtained as follows:

$$p(d) = 1 - \left(1 - \frac{1}{2} \exp^{-\frac{\gamma(d)}{2}}\right)^{8f} \quad (7)$$

where f is the frame size, d is the transmitter-receiver distance, $\gamma(d)$ is the signal to noise ratio (SNR).

We have conducted a comprehensive set of simulation experiments under Matlab to study the correlation between cumulative PER and PSNR values as presented in Section 4.1. We then conducted various performance tests to analyze the effectiveness of the EC scheme for different network design forces. Finally, we have validated our results on a real testbed with Tmote Sky wireless sensor nodes as explained in Section 5.

In the simulation experiments, we used thirty different grayscale test images of size 256×256 pixels for quality estimation. The results for only five different images are given due to the size constraints in the graphics. However, the results for the other images were similar to the ones that are presented.

4.1 Image Quality Estimation

For image quality estimation, thirty test images are impaired under a certain percentage of the packet loss. Then, the quality of the impaired images are evaluated in terms of PSNR for NC and EC schemes. A regression analysis is performed on the results as follows:

For NC: first, PSNR values vs PER are drawn onto a scatter plot as shown in Figure 5. The least-squares, fit through the points, are calculated by using a logarithmic equation as a function of (x) ; i.e number of lost packets. The regression equation for Lena image is calculated as:

$$PSNR_{NC} = -4,375 \ln(x) + 41,502 \quad (8)$$

Where the regression value that reflects the proportion of variation explained by the regression curve for Lena image is 0.99. Since the same curve fitting with close variations for all test images are obtained we can generalize the above formula for NC as:

$$PSNR_{NC} = \alpha \ln(x) + \beta \quad (9)$$

where α is a constant, which can be obtained through curve fitting over empirical data and β is the reference quality value of the image in the case of a single block loss. In the calculation of β , firstly, every possible single block of the image is

lost, then quality of the impaired image is calculated in terms of PSNR. Then β is acquired by taking the average of the PSNR values.

For EC: the effect of EC algorithm on the quality of the received image is evaluated by taking the same steps as explained above. Again, the results for five images are given in Figure 6. The regression equation obtained for Lena image (with proportion of variation 0.97) is given as:

$$PSNR_{EC} = -0,0032x + 31,63 \tag{10}$$

Due to similar behavior with close variations in all test images, the above equation can be generalized for EC as follows:

$$PSNR_{EC} = \alpha'x + \beta' \tag{11}$$

where β' is the quality of the watermarked image in case of a single block loss of the watermarked image and α' is a constant obtained from the empirical tests. As can be seen from the scatter plots and the equations (9) and (11),

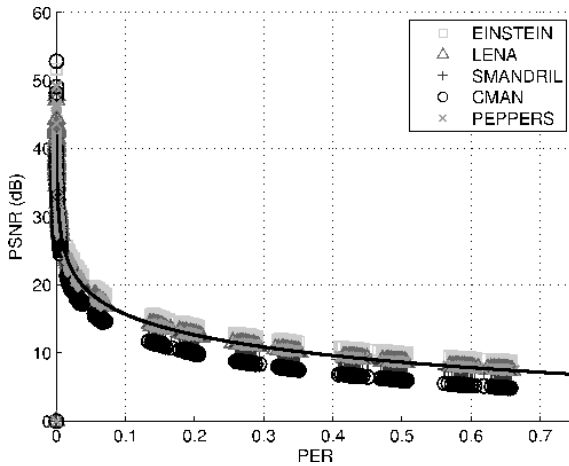


Fig. 5. Scatter plot of PSNR vs. PER and logarithmic least squares fitted curve for transmitted raw images

the relationship between the number of lost packets and PSNR is converted to a linear function with EC algorithm. Moreover, the algorithm achieves image quality over 25dB when PER is less than 0.6 for all test images.

The equations (9) and (11) can further be generalized for a multi hop path by replacing x with equation (6) as given below:

$$PSNR_{NC} = \alpha \ln(N[1 - (1 - p)^{n_h}]^{n_p}) + \beta \tag{12}$$

$$PSNR_{EC} = \alpha'(N[1 - (1 - p)^{n_h}]^{n_p}) + \beta' \tag{13}$$

These equations are also verified with the testbed results in Section 5.

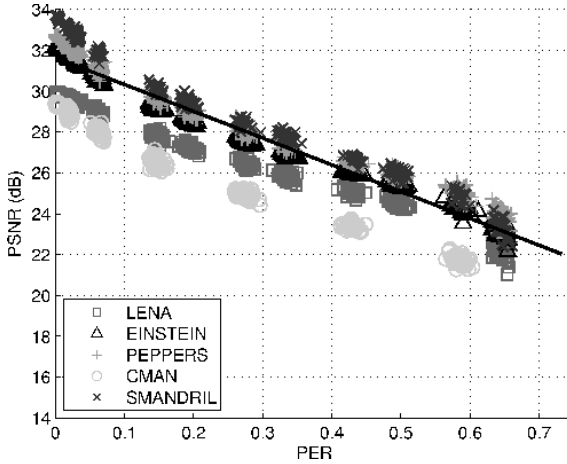


Fig. 6. Scatter plot of PSNR vs. PER and logarithmic least squares fitted curve for transmitted watermarked images

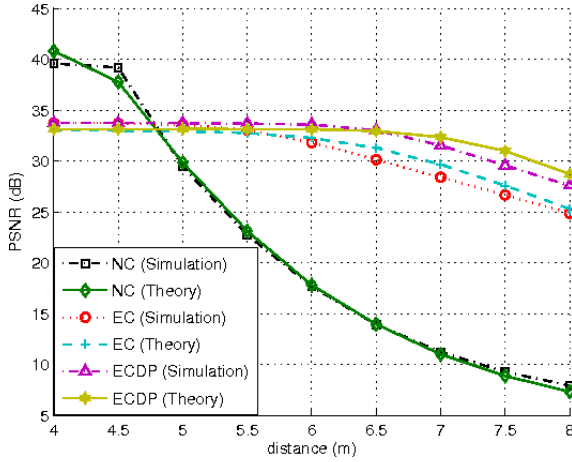
4.2 Performance Analysis

In this section, we present simulation and theoretical estimation results for NC, EC and ECDP schemes in terms of PSNR. For each test image, we run the simulations 50 times and obtain PSNR values together with the number of lost packets. We take the mean of these values as the result of the test. We then feed the number of lost packets to the equations (12) and (13) to obtain the corresponding theoretical estimation results. Estimated PSNR values are also plotted in the Figures so that the correlation between the real and estimated results can be seen.

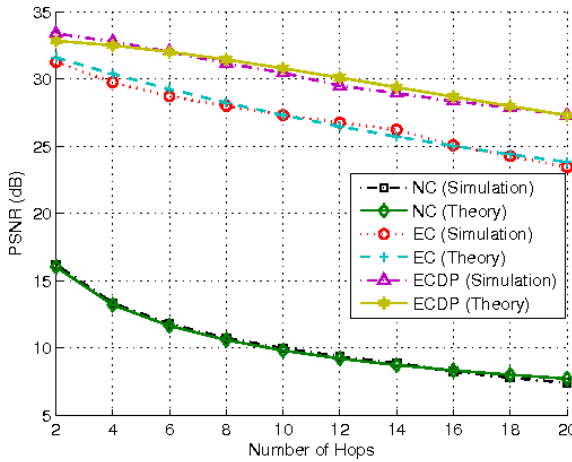
Figure 7(a) shows the impact of the physical channel in terms of internode distances on the PSNR performance. The results show that NC scheme is the most susceptible scheme to channel impairments. It is also clear that NC scheme is not adequate to transmit images over WMSN. EC and ECDP schemes are more robust to packet losses. For EC scheme, PSNR slowly decreases from 34 dB to 25 dB for varying distances. Figure 7(b) illustrates the PSNR performances versus number of hops, when the distance between nodes is 6m. Range of improvement over NC is changing from 17 dB to 20dB when the distance between hops is 6m. Performance gain attained by integrating the EC and disjoint multipath transmission schemes is at most 4dB. Hence, the performance is not profoundly improved by ECDP.

5 Testbed

In order to verify the results of the simulations, we have established an indoor, 10-hops testbed by using 20 Tmote Sky sensor nodes [20]. We utilized TinyOS



(a) PSNR vs. Distance ($n_h=1$).



(b) PSNR vs. Number of Hops ($d=6m$).

Fig. 7. Simulation Performance

v2.1 with nesC v1.3 [21] to realize a simple still-image transmission over a chain topology.

5.1 Node Deployment

We aim to achieve a clear line of sight between nodes and make them share the same communication medium to homogenize environmental effects on the communication channels. Therefore the tests are conducted inside a building with a large atrium as shown in Figure 2. Moreover, the nodes are partitioned into two groups (Group0 and Group1) and lined up vertically on thin linear sticks which

are horizontally pointed out from the windows on the first floor, approximately 5m above from ground, with no obstacles between them. The distance between the groups is measured as 27m. The groups consist of five "hop couples" with intra and inter couple spacings of 4 and 17cm respectively. As depicted in Figure 8, the sticks equipped with the sensors nodes are positioned parallel to each other to complete a hypothetical rectangular area when looked from above. The output power of nodes is set to -3dBm. Each group is connected to a base station computer via self-powered USB hubs, in order to avoid performance variation due to power differences when they run on batteries.

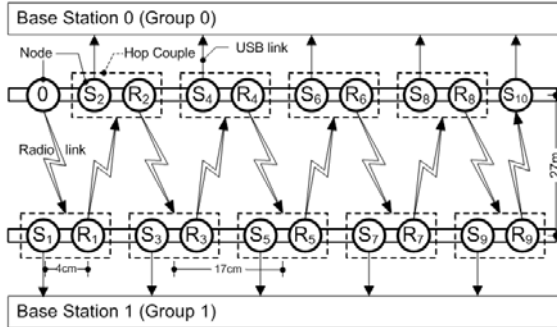


Fig. 8. Testbed Diagram

5.2 Image Transmission Setup

The actual image transmission scheme is as follows: A gray scale image, encoded with our EC algorithm, of 256x256 size is partitioned into 4x4 macro-blocks of 16B with extra 2B being used for the block offsets and sent over ten hops to the sink node. To make hop based PSNR comparisons accurately, it is necessary to get the packet loss patterns occurred in each hop at the same time, as conducting the tests on different time periods, and consequently on different diurnal conditions, causes dramatic changes in packet loss patterns. In the afternoon, for instance, we get very high PERs due to the noise induced by the crowd in the atrium, on the contrary, in the midnight we get low PERs. To satisfy these concurrency requirements, while transmitting an image over ten hops we record the intermediate results in each hop by using *snooping nodes*. In our image transmission scheme each hop consists of two nodes called "hop couple" which have the same node-id. In each hop couple, one of the nodes, called relay node (R_i , $i=0, 1 \dots 9$), is used to send the incoming data to the other hop couple with consecutive node id via radio link, while the other node, called snooping node (S_i , $i=1, 2 \dots 10$), is used to send the incoming data to the base station computer via USB link. There are only single nodes numbered with 0 and 10, as the source and the sink node respectively. The base station computers at each side records the image data along with RSSI (Received-Signal-Strength-Indicator) and LQI (Link-Quality-Indicator) values for each packet at each hop. To make more equitable comparisons of our EC algorithm for different images, the acquired image

loss patterns are used as masks and projected to the other encoded test images, instead of repeating the tests for them. After the projections, the resulting images are decoded with our EC algorithm. The block diagram of this operation is given in Figure 9.

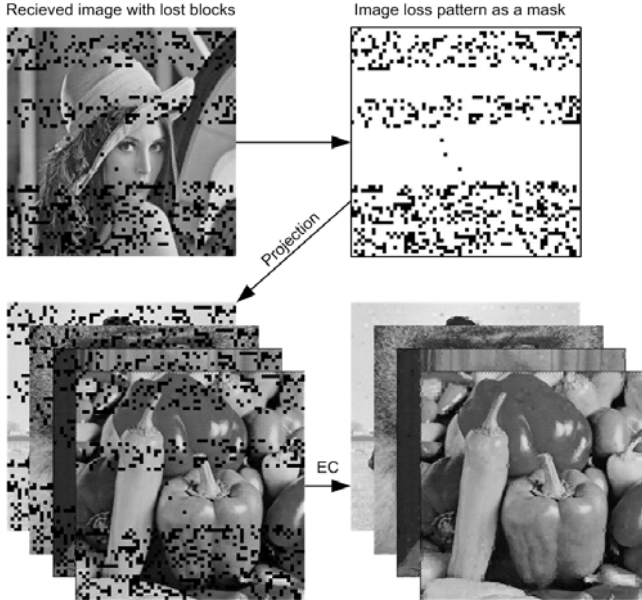


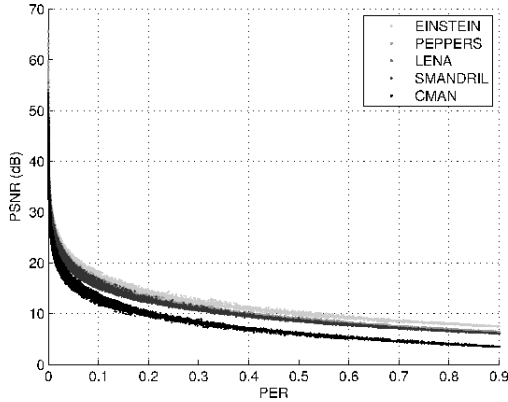
Fig. 9. Using image loss patterns as masks

The difficulties to establish a test setup for disjoint paths in a building with the requirements above, lead us to use another method to realize the tests for ECDP scheme. In this method, the tests taken place at the two different days are matched, and the images are fused as if they are coming from disjoint paths. Again, image loss patterns are extracted from the resulting images and projected to the other images as masks.

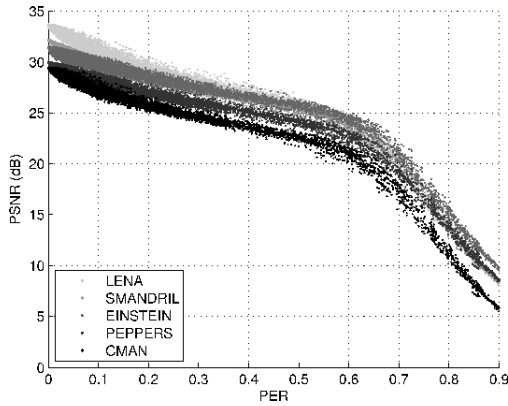
5.3 Testbed Results

We have conducted over 3000 image transmission tests spreading approximately 15 days. Over 30000 image loss patterns are gathered via 10 hops. The graphs, which show PSNR and PER relation for NC and EC scheme in Figure 10(a) and Figure 10(b), include all the results projected to five different images. It is obvious that the results of the real tests verify the simulation results depicted in Figure 5 and Figure 6. The results for EC scheme give us a threshold for PER as 0.6 to transmit an image within an acceptable quality.

To evaluate the effect of the number of hops on image transmission for all schemes, one-day-long tests within our result set are used. Only the tests from



(a) NC scheme



(b) EC scheme

Fig. 10. Scatter plot of PSNR vs PER for on testbed ($d=27m$)

holiday days are used to avoid variance in packet loss patterns due to environmental changes. In the tests packet reception rates vary from 0.77 to 1.00. The values coming from real tests were applied to the equations (12) and (13) to obtain the theoretical results. Figure 11 shows the real results for all schemes combined with the theoretical calculations. Figure 12 represents the channel conditions of the testbed in terms of average LQI. Because the chosen channel conditions for the simulations are worse than the testbed conditions, the results are parallel to the simulations in short distances. The results of real tests again indicate the superior performance of EC scheme over NC scheme. And also by using ECDP scheme, a little gain can be achieved over EC scheme.

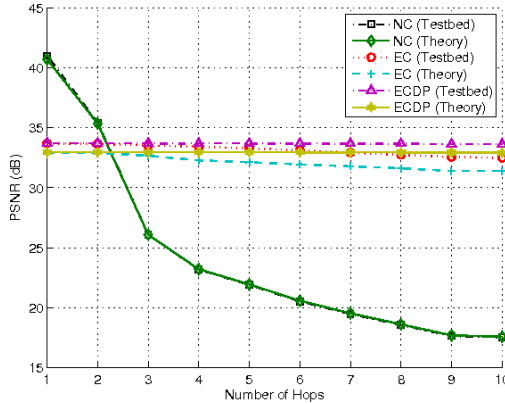


Fig. 11. PSNR vs Number of Hops on testbed ($d=27m$)

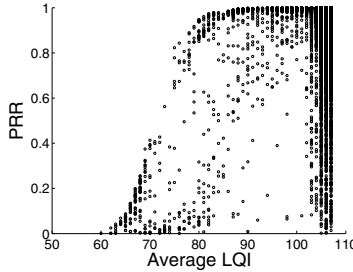


Fig. 12. PRR vs. Average LQI

6 Conclusion

We have shown that there is a correlation between PSNR values and the number of lost packets in a multi hop WMSN. Additionally, we have shown that when EC technique is used, PSNR value of the transmitted image is a linear function of the packet loss rate. Based on this theoretical relation, image quality requirements can be met by a transport protocol which statistically controls the cumulative packet error rate and guarantees the minimum required number of packets to be received at the sink.

We have also presented the effect of error concealment and multipath transmission on the quality of the raw images transmitted over WMSN. The simulation and real testbed results indicate that the EC algorithm is capable of restoring corrupted images, especially for high channel error conditions. Moreover, employing disjoint multipath transmission along with fusion at intermediate nodes brings further improvements on the received image quality.

References

1. Akyildiz, I., Melodia, T., Chowdhury, K.: A survey on wireless multimedia sensor networks. *Computer Networks* 51, 92–960 (2007)
2. Chow, K., Lui, K., Lam, E.: Efficient Selective Image Transmission in Visual Sensor Networks. In: *IEEE 65th VTC*, pp. 1–5 (2007)
3. Chen, M., Leung, V., Mao, S., Yuan, Y.: Directional geographical routing for real-time video communications in wireless sensor networks. *Computer Communications* 30, 3368–3383 (2007)
4. Dai, R., Akyildiz, I.F.: A spatial correlation model for visual information in wireless multimedia sensor networks. *Trans. Multi.* 11, 1148–1159 (2009)
5. Lee, H., Tessens, L., Morbee, M., Aghajan, H., Philips, W.: Sub-optimal Camera Selection in Practical Vision Networks through Shape Approximation. In: *Blanc-Talon, J., Bourennane, S., Philips, W., Popescu, D., Scheunders, P. (eds.) ACIVS 2008. LNCS, vol. 5259*, pp. 266–277. Springer, Heidelberg (2008)
6. Barr, K., Asanovic, K.: Energy-aware lossless data compression. *ACM Transactions on Computer Systems (TOCS)* 24, 291 (2006)
7. Wu, H., Abouzeid, A.: Energy efficient distributed JPEG2000 image compression in multihop wireless networks. In: *IEEE ASWN*, Citeseer, pp. 152–160 (2004)
8. Lee, D., Kim, H., Rahimi, M., Estrin, D., Villasenor, J.: Energy-efficient image compression for resource-constrained platforms. *IEEE Transactions on Image Processing* 18 (2009)
9. Pekhteryev, G., Sahinoglu, Z., Orlik, P., Bhatti, G.: Image transmission over IEEE 802.15. 4 and ZigBee networks. In: *IEEE ISCAS*, pp. 3539–3542 (2005)
10. Wu, H., Abouzeid, A.: Power aware image transmission in energy constrained wireless networks. In: *ISCC*, pp. 202–207 (2004)
11. Ferrigno, L., Marano, S., Paciello, V., Pietrosanto, A.: Balancing computational and transmission power consumption in wireless image sensor networks. In: *IEEE VECIMS*, p. 6 (2005)
12. Lin, S., Costello, D.: *Error control coding: fundamentals and applications*. Prenticehall, Englewood Cliffs (1983)
13. Zorzi, M.: Performance of FEC and ARQ error control in bursty channels under delay constraints. In: *48th IEEE VTC*, vol. 2 (1998)
14. Thomos, N., Boulgouris, N., Strintzis, M.: Optimized transmission of JPEG2000 streams over wireless channels. *IEEE Transactions on Image Processing* 15, 54–67 (2006)
15. Zhu, Q., Wang, Y.: *Error Control and Concealment for Video Communication*. In: *Visual Information Representation, Communication, and Image Processing* (1999)
16. Sarisaray, P., Gur, G., Baydere, S., Harmanc, E.: Performance Comparison of Error Compensation Techniques with Multipath Transmission in Wireless Multimedia Sensor Networks. In: *15th MASCOTS*, pp. 73–86 (2007)
17. Kundur, D., Hatzinakos, D.: Digital watermarking for telltale tamper proofing and authentication. *Proceedings of the IEEE* 87, 1167–1180 (1999)
18. Kundur, D., Hatzinakos, D.: Toward robust logo watermarking using multiresolution image fusion principles. *IEEE Transactions on Multimedia* 6, 185–198 (2004)
19. Zuniga, M., Krishnamachari, B.: An analysis of unreliability and asymmetry in low-power wireless links. *ACM Transactions on Sensor Networks (TOSN)* 3, 7 (2007)
20. Crossbow, T.: *TelosB Data Sheet*, <http://www.xbow.com/>
21. Department, U.B.E.: *TinyOS: An operating system for sensor networks*, <http://www.tinyos.net/>